International Journal of Automotive Technology, Vol. ?, No. ?, pp. ?–?(year)

TOPOLOGICAL ANALYSIS OF POWERTRAINS FOR REFUSE-COLLECTING VEHICLES BASED ON REAL ROUTES

PART I: HYBRID HYDRAULIC POWERTRAIN

F. SORIANO[1) *], M. MORENO-EGUILAZ[2)], J. ALVAREZ[3)] and J. RIERA[4)]

[1)]R&D Department of the Ros Roca Group, Av Cervera s/n, Tàrrega (Lleida) 25300, Spain
[2)]Center Innovation Electronics. Motion Control and Industrial Applications (MCIA). Technical University of Catalonia. Barcelona Tech., Rambla de Sant Nebridi 22, Terrassa 08222, Spain
[3)]Center for Engines and Heat Installation Research (CREMIT). Technical University of Catalonia. Barcelona Tech., Av. Diagonal 647, Barcelona 08028, Spain
[4)]Robotics and Industrial Informatics Institute (IRI). Technical University of Catalonia. Spanish National Research Council (CSIC), Llorens i Artigas 4-6, Barcelona 08028, Spain

(*Received date ; Revised date ;Accepted date*) * Please leave blank

ABSTRACT– In this two-part paper, a topological analysis of powertrains for refuse-collecting vehicles (RCVs) based on the simulation of different architectures (internal combustion engine, hybrid electric, and hybrid hydraulic) on real routes is proposed. In this first part, a characterization of a standard route is performed, analyzing the average power consumption and the most frequent working points of an internal combustion engine (ICE) in real routes. This information is used to define alternative powertrain architectures. A hybrid hydraulic powertrain architecture is proposed and modelled. The proposed powertrain model is executed using two different control algorithms, with and without predictive strategies, with data obtained from real routes. A calculation engine (an algorithm which runs the vehicle models on real routes), is presented and used for simulations. This calculation engine has been specifically designed to analyze if the different alternative powertrain delivers the same performance of the original ICE. Finally, the overall performance of the different architectures and control strategies are summarized into a fuel and energy consumption table, which will be used in the second part of this paper to compare with the different architectures based on hybrid electric powertrain. The overall performance of the different architectures indicates that the use of a hybrid hydraulic powertrain with simple control laws can reduce the fuel consumption up to a 14%.

KEY WORDS : Engines, Hybrid power vehicle, Energy management optimization, Drive cycle prediction

1. INTRODUCTION

The rising cost of oil production and the dependence of the transportation sector on fossil fuels, combined with the need for a rapid response to the global warming challenge, provide a strong impetus for the development of fuel-efficient vehicle propulsion systems. Hybridization is the only approach offering significant energy breakthroughs in the short and midterm.

* *Corresponding author*. e-mail: fsoriano@rosroca.com

This technological option is particularly interesting, although complex, when combining vehicles with significant weight, power, and drive cycles with a large number of starts and stops. This is the case of urban buses or refuse-collecting vehicles (RCV) (Ivanco *et al*., 2012, Dembski *et al*., 2005, Ivanič 2007, Soriano *et al*., 2014).

Compared with electric hybridization, hydraulic hybridization offers higher power density (more kW/kg and kW/m^3) but lower energy density (less kW·h/kg and kW·h/m^3) (Baseley *et al.*, 2007). Hydraulic hybridization seems to be the technical option which fits better into vehicles with high power flows such as heavy machinery. On the other hand, electric

hybridization seems to be the technical option which fits better into smaller vehicles such as sedan and family cars. Refuse-collecting vehicles and urban buses remain on an intermediate situation.

The main scope of this research is not to improve knowledge on hybrid hydraulic systems, which have been studied by other authors (M. Esfahanian *et al.*, 2013, Baseley *et al.*, 2012, Filipi and Kim 2010, Kim and Filipi 2007, Wu *et al.*, 2002, Wohlgemuth *et al.*, 2013, Surampudi *et al.*, 2009, Wu *et al.*, 2004, Bender *et al.*, 2013) in the past, but to study the impact of the use of this type of powertrains into RCVs. From an application point of view, commercial proposals are available in the market to hydraulically hybridize a powertrain in parallel (Bosch 2012), in series (Parker 2013) or by using two powertrains applied on different vehicle wheels (Proclain 2015).

In a previous work (Soriano *et al.*, 2014), fuel consumption modelling of refuse-collecting vehicles powered from an ICE have been proposed and their accuracy estimated on real routes.

In another recent work (Soriano *et al.*, 2015), specific algorithms have also been developed to identify the driving mode in real time in which the vehicle is running, which is closely related to the power consumption mode.

In this work, these energetic models are used to design powertrain architectures and estimate the efficiency of these topologies on a set of real routes. The algorithms to identify the driving mode in real time are also tested to measure its contribution to the powertrain efficiency.

The present work is organized as follows: first, a data-logging system, that it is used to register the routes in which the powertrain models are tested, is introduced. Second, a general investigation, to understand how an ICE is working in regular cycles, is presented and the potential of powertrain hybridization is analyzed. Third, the drive cycles, in which the powertrain model will be tested, are presented and some of their singularities are explained. Fourth, the ICE and the hybrid hydraulic powertrain models are analyzed and their components are defined one by one. Fifth, the artificial intelligence system which estimates in which driving mode the powertrain is operating is mentioned, despite the fact that it is not developed in the present work but in a previous one (Soriano *et al.*, 2015). Sixth, the calculus engine, which has been developed specially for this work, is disclosed and its estimation details are presented. Finally, the performance of the ICE-based powertrain and the hybrid hydraulic powertrain models is estimated on real routes using the proposed calculus engine. The results are discussed with relevant conclusions.

2. REFUSE-COLLECTING VEHICLES AND DATA ACQUISITION SYSTEM

A refuse-collecting vehicle is a heavy vehicle that contains a mobile machine (a refuse container lifter and a refuse compactor, hereinafter referred to as “the body ancillaries”). As they are energized from a single engine, the powertrain must deliver energy with two purposes, the first one is for the vehicle traction, and the second one is to power the body ancillaries.

An automotive data acquisition system (Soriano *et al.*, 2014) is installed on board to collect all the data that are potentially interesting to model the energy consumption of both the body ancillaries and the vehicle traction. To avoid interferences in the regular work of vehicle drivers and operators, this system is installed in places rarely reached by the workers. The on-board data-logging kit is composed of:

- CAN Data logger: CANalyzerCANCase XL with two CAN ports (SN 007130-011289)
- PLC: IFM CR0505 (SN 024137). Analogue channel resolution 12 bits, resolution ±1.0% FS
- GPS: RM Michaelides CAN link 2105 (part no. 253004018), full scale 0.00001º L/l, 0.1-m height, CEP 3.5 m
- Inclinometer: STW YNGS1ST2 with CAN Open port (part no. 080537682003). Range ±6g resolution 0.2 mg.
- Two pressure sensors IFM 9021 (SN 12911 A) Range 0.250 bar, ±0.25 BFSL, ±0.5LS.

Figure 1. Detail of the data acquisition system: GPS Module (upper left), GPS Antenna (upper right), CAN Case XL (below left), and Inclinometer (center right).

Figure 2. Detail of the data acquisition system wiring.

The first port of the CAN data logger is connected to the J1939 CAN bus of the vehicle; no filters are implemented on this port so all the information available is logged.

The second port is connected to a small CANOpen network, consisting of a GPS device, a PLC with CAN ports for mobile applications, and an inclinometer. The two pressure sensors are plugged to the hydraulic circuits of the body ancillaries (compactor and lifter) and wired to the analogue inputs of the PLC. The values read are sent into the CANOpen network.

Using the data-logging kit, a significant quantity of data was collected every day from a single RCV from April 2013 to June 2013 in Barcelona. The data were afterwards post-processed using software based on Matlab (Soriano *et al.*, 2014).

3. CHOSEN DRIVE CYCLES

Table 1 shows the list of routes logged with the described data-logging kit and chosen for powertrain simulations.

Table 1. Parameters of the logged routes.

Route	Total Distance (km)	Total Time (min)	Total collected bins/containers (units)
1	73.9	460.8	183
2	72.7	470.9	175
3	71.3	392.8	166
4	69.0	422.3	163
5	67.6	406.5	144
6	70.6	421.5	161
7	69.9	471.1	169
8	70.5	480.7	163
9	67.8	421.1	168
10	67.8	423.5	160
11	76.6	465.0	194
12	67.2	428.1	166
13	73.7	460.2	184
14	68.4	471.6	169
15	82.0	542.3	266

These routes were registered in a regular RCV service in Barcelona (in the areas: Bordeta, Spain Square, Poble-Sec, Paral·lel), the experimental data shows the maximum slope is lower than 7% and the maximum vehicle acceleration value is 1.4 m/s^2.

Routes numbered from 1 to 14 represent routes without abnormal situations. The route numbered 15 belongs to a route in which the vehicle had to operate as a rescue vehicle. This means that after finishing its regular route, it had to substitute another vehicle, which suffered a breakdown and had to come back to the base with its route unfinished and the refuse not collected.

4. ANALYSIS OF THE INTERNAL COMBUSTION ENGINE

To understand the efficiency improvement potential of the powertrain hybridization, two algorithms have been developed to analyze the operation of the internal combustion engine in a standard RCV powertrain. The ICE studied with the first algorithm is a 200-kW natural gas unit.

The first algorithm registers the torque (J1939 SPN 513) and RPM (J1939 SPN 190) of the ICE, acquiring data at 10 Hz during the whole working route. By plotting the logged data on a graphic (see Figure 3), the density of samples at each RPM (abscissa) and torque (ordinate) can be observed. The coloured areas in red mean a high density sample, while the coloured areas in blue mean a low density sample.

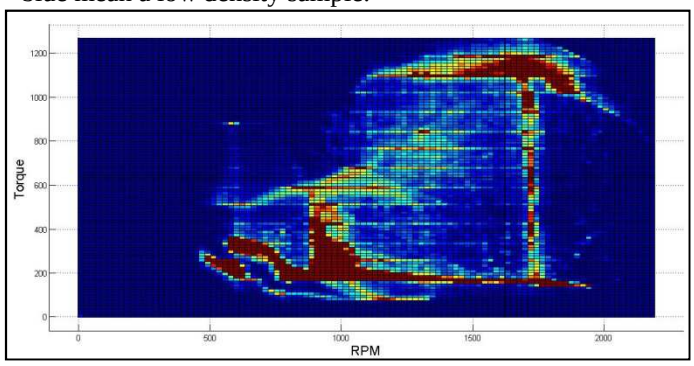

Figure 3. Densities of samples.

In Figure 3, three areas containing a higher density sample can be clearly identified. These three areas have been marked with red balloons on Figure 4:

The first area, labelled as 1, belongs to the samples when the ICE has been idle (vehicle stopped due to traffic or waiting to collect refuse). This area has the highest number of samples of all identified areas.

The second area, labelled as 2, belongs to the samples when the vehicle is stopped but the body ancillaries are working. No traction power is needed but power to

energize the body is consumed. This is the area with the second highest number of samples.

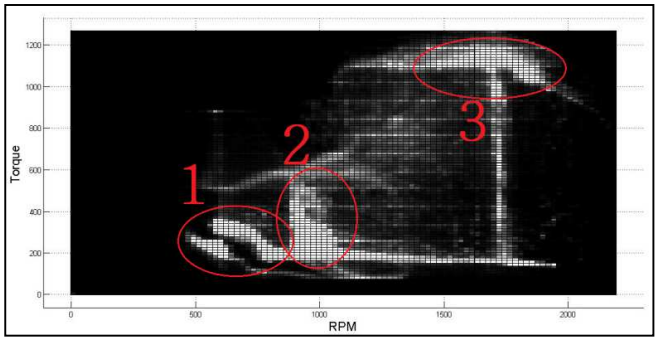

Figure 4. Some identified areas with high density of samples.

The third area, labelled as 3, belongs to the interval of time when the vehicle is being driven from one stop to another. Usually this manoeuvre is performed at full throttle. This is the area with the third highest number of samples.

In Figure 5, the efficiency map of the gas engine is shown over Figure 3. The isoconsumption trajectories/lines can be appreciated with the associated fuel consumption values.

Comparing the areas with high density samples (Figure 3) with an efficiency map (Brake Specific Fuel Consumption/BSFC in g/kWh) as in Figure 5, it must therefore be concluded that the ICE of a standard RCV working on a regular refuse-collecting route tends to work far from the high efficiency points.

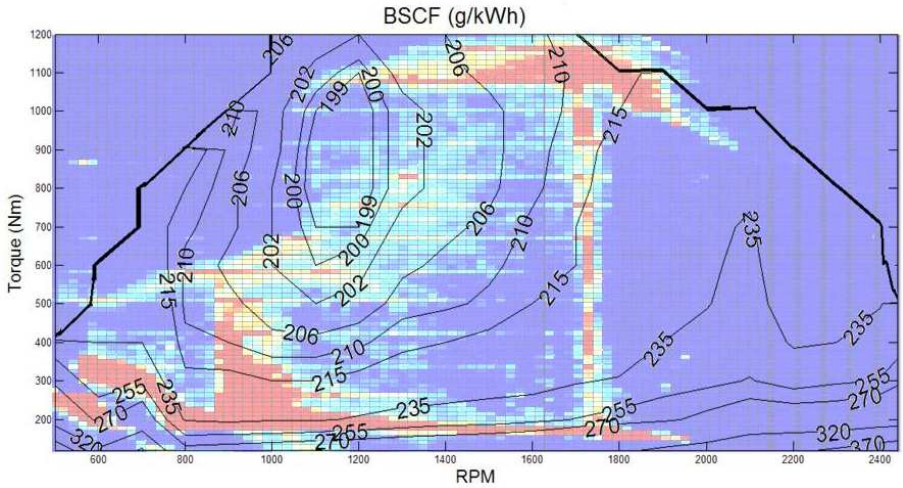

Figure 5. BSFC (g/kWh) of a 200-kW gas engine.

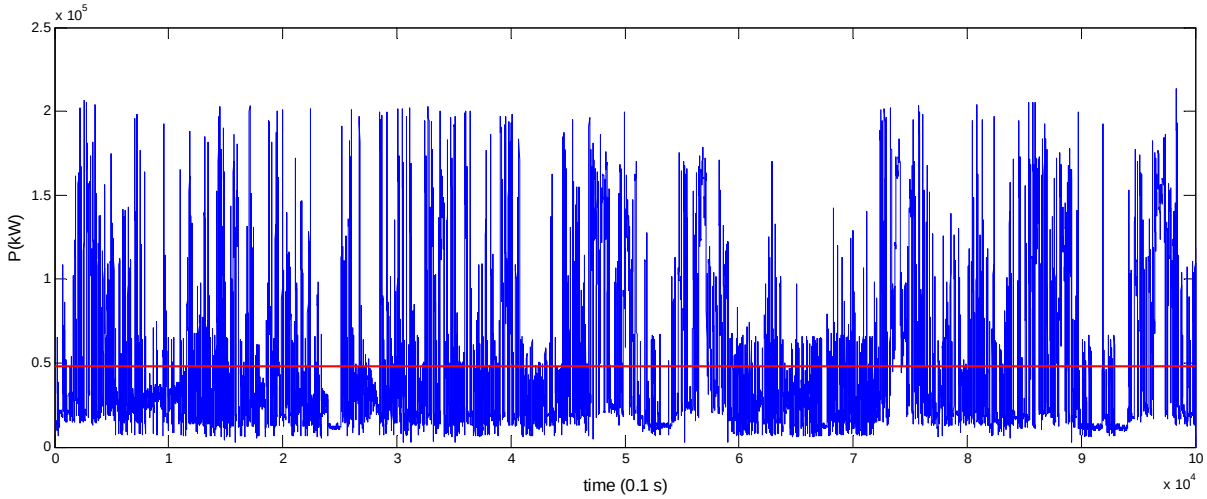

Figure 6. Instantaneous power (in blue) and average power (in red) [kW] for an RCV drive cycle.

The second developed algorithm to analyze the ICE operation estimates the instantaneous engine power and also its average value from the previously mentioned engine RPM and torque, during the whole collecting cycle and plots both versus time. The studied ICE is a 220-kW diesel unit. In Figure 6, the instantaneous power (in blue) and its average value (in red) can be observed for a whole refuse-collecting drive cycle.

Despite the fact that maximum peak power values are over 200 kW, the average value of power is from 40 kW to 70 kW for the complete set of analyzed routes.

The main conclusions of this section are that the ICE hardly ever works at high efficiency points and it works far from the maximum power points most of the drive cycle. A series hybrid vehicle can maintain its engine working at high efficiency points independently of the total instantaneous power demanded by the powertrain or its speed. This has demonstrated that a series hybrid vehicle is more efficient in similar drive cycles such as urban buses (Zhengce 2009). For this reason, it is decided in this paper that a series hybrid vehicle be chosen as powertrain architecture.

5. HYDRAULIC VEHICLE MODEL

The proposed powertrain architecture in this work is composed of three main elements: a hydraulic accumulator as the energy storage system (ESS), an ICE as the energy generation system (EGS), and a hydraulic motor/pump as the energy consumption/generator system (ECS).

In Figure 7, the proposed topological design in this work is introduced. The cardan of the vehicle is linked to the hydraulic motor of the vehicle through the gearbox which remains the same as in the original vehicle (with ICE).

Depending on the position of the directional valve, the 'Variable Displacement 2-Way' element, the hydraulic motor will act as motor or as pump, consuming power from the 'High Pressure Line' or adding power to the 'High Pressure Line'. This schema does not intend to be an exhaustive design but a conceptual proposal which will help to understand the hybrid powertrain architecture.

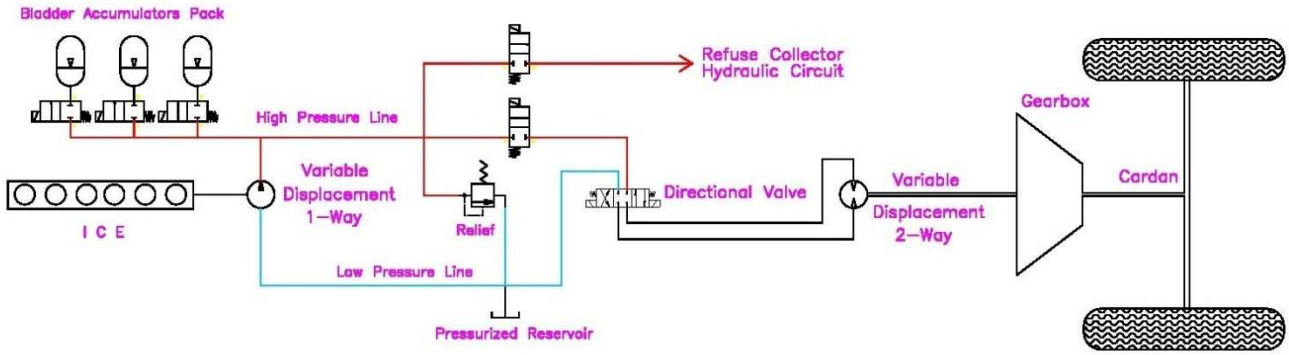

Figure 7. Series architecture of the proposed hybrid hydraulic powertrain.

5.1. Hydraulic Motor and Pump Model

The motor/pump model proposed (referred on Figure 7 as 'Variable Displacement 1- or 2-Way) is an electronically controlled variable displacement motor-pump with fixed stroke pistons and electronically-controlled digital valves (no swash plate or bent axis), (Wadsley 2011). The main reason for working with this technologic concept is that the hydraulic motor can match any pressure at the high pressure rail with any torque needed at the input axe of the gearbox, just modifying the displacement of the pump (of course, there will always be limits on the pump displacement). At the same time, its efficiency is higher at a wider RPM range compared with the traditional concept of variable displacement pumps (Wadsley 2011).

In the associated model, the efficiency of the motor and motor/pump is taken directly from the efficiency maps proposed in (Wadsley 2011) or interpolated for intermediate displacement values.

5.2. Hydraulic Accumulators

The model of the hydraulic accumulator is inspired in the work published in (Baseley *et al.*, 2007). More complex and accurate models (Y. L. Chen *et al.*, 2012 , Kim and Filipi 2007) have not been considered because, as mentioned previously, the main goal of this work is not to have an exhaustive hydraulic model but to

estimate the impact of a hydraulic powertrain on an RCV.

The size of the accumulators has been estimated fulfilling the manufacturer requirements (Hydac 2013). The whole proposed system is a bladder accumulator, whose behaviour is supposed to be adiabatic, filled with nitrogen. The expression used to calculate the accumulator sizing is:

$$V_0 = \frac{\Delta V}{\left(\frac{P_0}{P_1}\right)^{0.714} - \left(\frac{P_0}{P_2}\right)^{0.714}} \quad (1)$$

Where:
P_0: Gas pre-charge pressure (bar).
P_1: Lower working pressure (bar).
P_2: Higher working pressure (bar).
ΔV: Volume at P2 – volume at P1 (m^3).
V_0: Effective gas volume (m^3).

The expression used to estimate the inner pressure from the accumulated volume is:

$$P_X = P_1\left(\frac{V_1^{1,4}}{V_x^{1,4}}\right) \quad (2)$$

and the expression used to estimate the energy stored in a compression between any two states 1 and 2 is:

$$E(kJ) = \frac{P_1 V_1^{\gamma}}{1000}\left(\frac{V_2^{1-\gamma} - V_1^{1-\gamma}}{1-\gamma}\right) \quad (3)$$

P_1: Lower working pressure (bar).
V_x: Effective gas volume at status x (m^3).

The efficiency of this system is always difficult to estimate because it depends on the heat exchange with the environment. As the vehicle speed and the ambient temperature change, the convection coefficient is difficult to estimate. In this work, the efficiency of the hydraulic accumulator used for calculations is 0.9 (Baseley *et al.*, 2007). This is implemented in the model applying the corresponding pressure loss on the discharge phase of the accumulator (Baseley *et al.*, 2007), as represented in Figure 8.

5.3. Body Hydraulic System

The model of the body of the RCV used for estimations is a Ros Roca Cross Body with a Ros Roca UPC lifter (both hydraulically powered). In this work, the body ancillaries' energetic consumption is simplified to its pressure and flow consumption. The pressure is taken from a pressure sensor installed on the hydraulic line at the output of the oil pumps as in (Soriano *et al.*, 2014). The flow (4) is estimated considering the RPM of the engine (J1939 SPN 190); the displacement of the pump (D, cc/rev) and its leakage. The leakage is estimated as in (Soriano *et al.*, 2014) using the maps provided by the pump manufacturer.

$$Q = (RPM \cdot 60 \cdot D) - \text{Leakage} \quad (4)$$

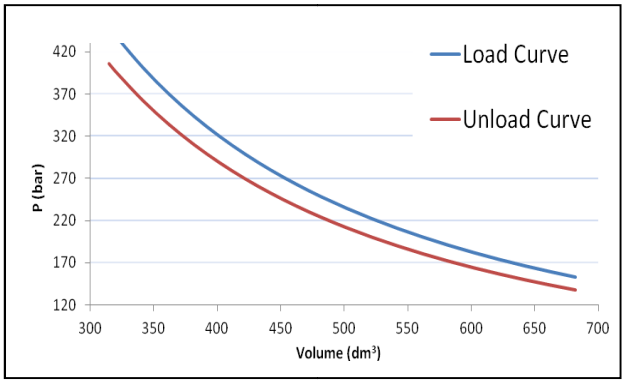

Figure 8. Graphic representation of the load and unload curve of the bladder accumulator (adiabatic with 90% efficiency).

5.4. Internal Combustion Engine

In this paper, the engine element is reduced to the optimal consumption curve of the BSFC map (the gas engine in Figure 5) which will estimate the fuel consumption, the torque, and RPM in the function of the demanded power (see Table 2).

The fuel necessary to restart the engine when it is off has been parameterized and introduced in the simulation of the powertrain. As no specific literature for heavy duty engines has been found, this parameter has been taken from a smaller engine (Matsuura *et al.*, 2004) and its value corrected based on the displacement ratios (estimated to be 10.5 g for this study).

Table 2. Parameters of the optimal consumption curve of the ICE.

Power (kW)	33.72	46	56.5	73.3	97.9	113	127	144	162	184	196	207	219	220
Speed (RPM)	700	800	900	1000	1100	1200	1300	1400	1500	1600	1700	1800	1900	2000
BSFC (g/kW·h)	213	209	205	202	198	198	201	203	205	207	211	213	217	222
Torque Nm	460	550	600	700	850	900	930	980	1030	1100	1100	1100	1100	1050

6. ROUTE PREDICTION SYSTEM

RCV routes are characterized by two main working modes.

The first mode is the vehicle transport mode, in which the drive cycle is characterized by higher speeds and slower power transitions; this mode corresponds to the travel from the base to the urban zone and vice-versa, or from the urban zone to the landfill/transfer station and vice-versa. In this mode, the engine is usually working in the area marked as '3' in Figure 4.

The second mode is the refuse-collecting mode (performed in the urban zone). In this mode, the vehicle is accelerated and slowed aggressively from one bin collection to the next one. When the vehicle is stopped, the ancillaries are actuated. In this mode, the working points of the engine change constantly among the areas '1', '2', and '3' of Figure4.

Due to the fact that different RCV route segments have different power demand characteristics, the capacity to know in which RCV route segment the vehicle is working is an advantage for the management algorithms in case of hybrid power trains. The transport mode has typical power consumption values of 90 to 120 kW with no transients; the collecting mode has typical power consumption values of 17 to 25kW with significant number of transients.

In a previous work (Soriano *et al.*, 2015), detailed information about the drive cycles in an RCV can be found. An algorithm based on artificial intelligence (AI) is also proposed to identify if the vehicle is working in 'collecting mode' or 'transport mode'. In the present work, this information is assumed available.

7. ICE CONTROL STRATEGY

Based on the state of charge (SOC) of the accumulators and the 'Engine Status', the ICE control strategy (Figure 9 and Equations 5 to 8) is defined by a deterministic algorithm. The ICE control is inspired in (Kim and Filipi 2007) but parameterized, meaning that the parameters (SOC_{Limit}, SOC_{100}, P_{mean}) can be changed during the drive cycle depending on a higher layer control strategy.

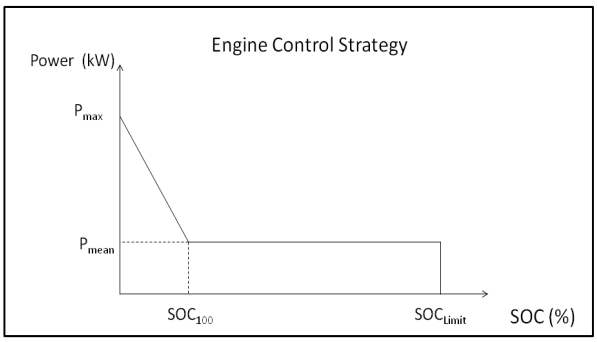

Figure 9. Control Strategy for the Internal Combustion Engine.

At the abscissa axis, the state of charge (SOC %) of the ESS is shown; at the ordinate axis, the power demanded to the engine is shown.

The ICE has two operating modes: running and stopped. When the SOC of the ESS reaches SOC_{Limit} (limit SOC value at which the engine can generate energy), the engine mode becomes stopped and it will be switched again to running mode only if the SOC falls below SOC_{100} (value below which the power demanded to the engine is increased proportionally reaching 100% power at SOC zero). When the ICE is stopped, it has no consumption and each time the ICE is started, it consumes the fuel amount specified in the engine model.

When the engine is running, it follows the following rules:

If the SOC of the ESS is between two values (SOC_{100} and SOC_{Limit}), the power demanded from the ICE is the average value of a drive cycle, or part of a drive cycle (P_{mean}).

In a previous work authors (Soriano *et al.*, 2015) identified RCVs have two main driving modes on their drive cycles: the refuse collection and the transport. The average power demand (P_{mean}) in the refuse collection mode was about 17 kW to 25 kW, the average power demand in the transport mode is about 90 kW to 120 kW, the average power demand of the whole service (including both modes) is between 40 kW to 70 kW. In this previous work authors also demonstrated that the driving mode can be identified by the use of neural networks.

If the SOC of the ESS is below SOC_{100}, the power demanded from the ICE will increase proportionally to the distance to SOC_{100}, reaching the maximum nominal power (P_{max}) of the ICE when the SOC is zero.

The following equations summarize the control algorithm used for the engine control:

$$if\left(Engine\_Status = ON\right)$$

$$if\left(SOC \le SOC_{100}\right),\ P(kW) = P_{mean} + \left(P_{\max} - P_{mean}\right)\left(SOC_{100} - SOC\right)/\ SOC_{100} \quad (5)$$

$$if\left(SOC_{100} < SOC < SOC_{Limit}\right),\ P(kW) = P_{mean} \quad (6)$$

$$if\left(SOC \geq SOC_{Limit}\right),\ P(kW) = 0 \qquad \text{and Engine Status = OFF} \tag{7}$$

$$elseif\left(Engine\_Status = OFF\right)$$

$$if\left(SOC \leq SOC_{100}\right),\ P(kW) = 0 \qquad \text{and Engine Status = ON} \tag{8}$$

$$if\left(SOC > SOC_{100}\right),\ P(kW) = 0 \qquad \text{and Engine Status = OFF} \tag{9}$$

8. COMPONENT SIZING AND PARAMETER TUNING

In this work, the parameters SOC_{100} and SOC_{Limit} have been set to 30% and 70%, respectively. The P_{mean} parameter will be controlled in two different ways, which will define two control strategies.

In the first powertrain control strategy, it is supposed that the AI system, which identifies the current driving mode (vehicle transport and refuse-collecting drive cycle), is unavailable. The neural network algorithms to do that identification were presented in a previous work (Soriano *et al*., 2015). As the average power (P_{mean}) of the whole drive cycle is between 40 kW and 70 kW in the previously analyzed cycles, and in this spectrum, the highest efficiency is found at 70 kW, this value is chosen as P_{mean}.

In the second powertrain control strategy, the AI system is available. The average power (P_{mean}) during the refuse-collecting mode is about 17 kW to 25 kW and the average value during the vehicle transport mode is about 90 kW to 120 kW. Using the same criteria previously mentioned, the P_{mean} is set to 25 kW during the refuse-collecting mode and to 100 kW during the transport mode.

As the bladder accumulators (ESS) are cheap components compared with the cost of an ICE or an RCV body, its cost has not been considered for the powertrain dimensioning, knowing that the main limitation of an RCV is its volume (the volume occupied by these components cannot be used to transport refuse which affects machine productivity):
Given that the bladder pack would be placed between the chassis cabin and the body, and the refuse body will have to be moved backwards, all this room will be filled with bladders, resulting to a final volume of 700 liters (7 bladders multiplied by 100 l/bladder). Pressures P0, P1, and P2 would be 153, 170, and 450 bar, respectively, which are the usual values for hydraulic circuits and are useful for the selected motor.

The hydraulic motor and pump have been sized according to the needs of an RCV powertrain as the one studied in this paper (maximum torque 1200 Nm and maximum speed 2450 RPM), which are the standard values for this type of technology. Commercial proposals with similar figures can be found in the market.

As the energy stored in hydraulic bladders is minimal (7760 kJ considering the previously mentioned volumes and pressures), a downsizing criteria cannot be applied to the internal combustion engine, and it has to deliver the same amount of power of the original ICE. As a result, the original ICE remains the same.

9. CALCULATION ENGINE

The calculation engine of this paper has been developed in Matlab.

Using data from the routes introduced in Table 1, two vectors (RPM and power) containing samples at 0.1 Hz during the whole collecting work (about 7 to 8 hours), have been generated daily for 15 days.

In the calculation engine, the ICE RPM and torque values were extracted from the logged and post-processed data.

Two different hardware architectures have been simulated, a standard ICE and a hybrid series powertrain.

For the standard ICE, at each time sample (at 0.1 s), the algorithm estimates:

The instantaneous power generated by the ICE, based on the logged data.

Based on the power and RPM, it searches the BSFC.

Multiplying the two previous values (power (kW) and BSFC (g/kWh)), it estimates the instantaneous consumption, which is integrated on the whole route to get the total fuel consumption.

To estimate both powertrains in the maximum possible equity conditions, the intervals of time when the powertrain is not generating useful energy (idle) have been set to zero consumption. This is representative of a start/stop vehicle.

For the hybrid hydraulic powertrain, at each time sample (at 0.1 s), the algorithm estimates:

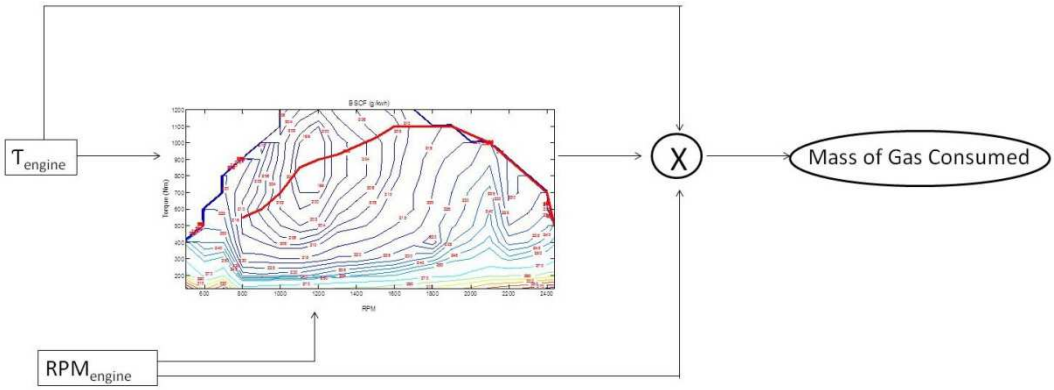

Figure 10. Detail of the ICE fuel estimation flow.

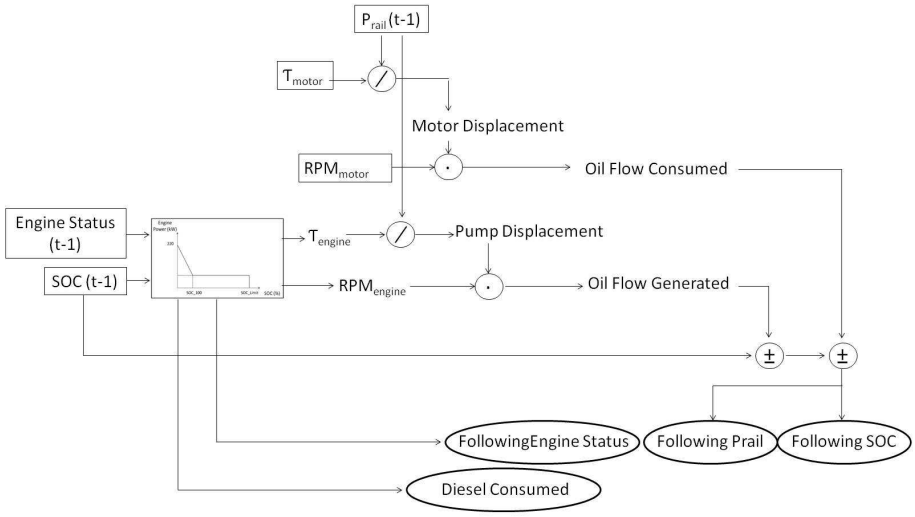

Figure 11. Diagram of the calculation engine.

The instantaneous power generated by the ICE, based on the SOC of the ESS in the previous instant. Based on the motor torque and the rail pressure, the displacement of the pump and the oil flow are estimated.

The instantaneous power consumption of the motor, based on the logged data. Using the instantaneous motor torque, the hydraulic rail pressure and the variable displacement of the pump, the pump displacement and the oil flow are estimated.

If the addition of the two previous values is negative, it means that there is lack of power that is supplied by the ESS. If it is positive, the power excess is stored on the ESS.

Figure 11 summarizes how the simulation process of the powertrain is implemented. Logged files corresponding to real routes are used to feed the algorithm which is executed in quasistatic mode. As the acquisition frequency was adjusted to 10 Hz, the file contains one register for each 0.1 s of the route.

The input parameters of the algorithm are displayed in boxes. The output parameters are showed in balloons.

The pressure at the high pressure line 'Prail' and the motor torque Tmotor' define the displacement of the hydraulic motor:

$$D(cm^3/rev) = \Gamma_{motor}\,(N\cdot m)/P_{rail}\,(Pa) \tag{10}$$

The displacement and the RPM of the motor define the 'Oil Flow Consumed' from the high pressure line.

$$Q\left(m^3/s\right) = RPM_{motor}\cdot\frac{D(cm^3/rev)}{60\cdot 10^6} \tag{11}$$

The pump displacement and the pump flow are estimated in the same way.

As mentioned previously, the simulation is executed in quasistatic mode so no transients on the engine, pumps or motor are considered. No models for the losses on the hydraulic lines have been considered.

The body ancillaries are designed to work at constant flow so they cannot be fed from the bladders, which would feed the ancillaries following an adiabatic

discharge curve which determines pressures instead of flows. When the vehicle is stopped and the ancillaries need power, they will be fed from the engine and pump at the nominal flow.

Based on the power generated by the engine and its BSFC map, the instantaneous fuel consumption is estimated.

The whole route consumption is approximated by integration, considering the initial SOC of the hydraulic ESS is 100%.

10. SIMULATION RESULTS

Table 3 summarizes the results of the simulations with different powertrains. In the first column, the route number according to Table 1 is displayed. In the second column, the result of the ICE consumption in kg for each route is shown at the bar's left. In the third column, the result of the Hybrid Hydraulic powertrain with no AI adaptation to the different driving modes can be found. In the fourth and last column, the result of the Hybrid Hydraulic powertrain with AI adaptation is presented.

To get an easier reading of Table 3, all their values have been reduced to the equivalent fraction of the ICE consumption, at the bar's right. In addition, the global average value for the 15 routes has been estimated and presented in Table 3.

Table 3. Fuel consumption (kg) of the different architectures.

Route	ICE (Fuel kg / Ratio)	Hybrid Hydraulic Powertrain without zone identification (Fuel kg / Ratio)	Hybrid Hydraulic Powertrain with zone identification (Fuel kg / Ratio)
1	34.51 / 1	30.86 / 0.89	29.59 / 0.86
2	33.05 / 1	29.93 / 0.91	28.76 / 0.87
3	33.08 / 1	31.37 / 0.95	30.40 / 0.92
4	29.49 / 1	26.16 / 0.89	25.06 / 0.85
5	29.53 / 1	27.13 / 0.92	25.85 / 0.88
6	31.25 / 1	28.45 / 0.91	27.30 / 0.87
7	30.98 / 1	25.80 / 0.83	25.15 / 0.81
8	31.67 / 1	26.59 / 0.84	25.52 / 0.81
9	30.76 / 1	27.38 / 0.89	26.37 / 0.86
10	30.81 / 1	27.62 / 0.90	26.54 / 0.86
11	34.76 / 1	32.21 / 0.93	30.99 / 0.89
12	31.13 / 1	28.00 / 0.90	26.96 / 0.87
13	33.15 / 1	31.05 / 0.94	29.71 / 0.90
14	32.10 / 1	28.20 / 0.88	27.18 / 0.85
15	39.24 / 1	32.39 / 0.83	31.10 / 0.79
Average	1	0.89	0.86

The energy supplied to the system from the ESS (estimated as SOC change between the start and end of the route), which is in fact replacing part of the fuel consumed, is not included in Table 3. After estimating these ESS energy consumption values they have been found to be clearly two orders of magnitude lower than the values of fuel energy consumption. Therefore, these terms have been neglected.

As mentioned previously, simulation has been executed in quasistatic mode, which means that the transients have not been modelled and some of the losses, such as intermediate positions on the directional valve, unfinished displacements of the variable displacement pumps, or pressure drops in the lines have been ignored because of representing a lower order of magnitude. Therefore, the results of the simulations should not be understood as a final value of the powertrain improvements but as an asymptotic value, i.e., the better the powertrain components' control strategy is, the closer the consumption results will be to these values.

It can be appreciated that the Hybrid Hydraulic powertrains, both with and without zone recognition, show relevant fuel efficiency improvements if compared when conventional powertrains.

11. ANALYSIS AND CONCLUSIONS

When comparing the ICE and the Hybrid Hydraulic without neural adaptation, the average efficiency improvement is about 10% to 11%. When comparing the Hybrid Hydraulic with neural adaptation, the average efficiency improvement is about 13% to 14%.

That means that most of the improvement is due to hardware modification. However, the implementation of the neural recognition system remains interesting because its implementation in an industrialized system has a very low cost (just software development and maintenance) and the impact is still meaningful in terms of fuel consumption.

With regard to its potential industrialization, the implementation of hybrid hydraulics is a very interesting option. On the one hand, there is a very deep experience in the implementation of these components in commercial vehicles and mobile machines. On the other hand, the fact of being series production components means that they will have low cost and high reliability, compared to components that are currently produced in smaller series such as supercapacitors or batteries (when batteries are not related to big series automotive applications).

Finally, the hybrid electric powertrain remains an interesting area to be studied, and the development of this study is the goal of the second part of this work.

REFERENCES

Artemis Intelligent Power Ltd. Personal communication. 2014

Baseley, S., Ehret, C., Greif, E., and Kliffken, M. (2007) Hydraulic Hybrid Systems for Commercial Vehicles, *SAE Technical Paper* 2007-01-4150.

Bender, F.A., Kaszynski, M., Sawodny, O. (2013), Drive Cycle Prediction and Energy Management Optimization for Hybrid Hydraulic Vehicles, in *Vehicular Technology, IEEE Transactions on*, **62**, **8**, 3581-3592.

Bosch Rexroth (2012). Hydrostatic regenerative braking System HRB. RE 94850/10.2012.

Dembski, N., Rizzoni, G., Soliman, A., Fravert, J. *et al*. (2005) Development of Refuse Vehicle Driving and Duty Cycles. *SAE Technical Paper*. 05-01-1165.

Esfahanian, M., Safaei, A., Nehzati, H., Esfahanian, V., Tehrani, M. M. (2014). Matlab-based modeling, simulation and design package for Eletric, Hydraulic and Flywheel hybrid powertrains of a city bus, Int. J.*Automotive Technology* 15, 6, 1001-1013.

Filipi, Z. and Kim, Y. J. (2010). Hydraulic Hybrid Propulsion for Heavy Vehicles: Combining the Simulation and Engine-In-the-Loop Techniques to Maximize the Fuel Economy and Emission Benefits. *Oil & Gas Science and Technology* - Rev. IFP, 65 155-178.

Hydac (2013). Sizing Accumulators. Innovative Fluid Power PN#02068195/04.13/ACU1102-1326.

Ivanco, A., Johri, R. and Filipi, Z (2012). Assessing the Regeneration Potential for a Refuse Truck Over a Real-World Duty Cycle. *SAE Int. J. Commer. Veh*. 5(1):364-370.

Ivanič, Ž. (2007). Data Collection and Development of New York City Refuse Truck Duty Cycle. *SAE Technical Paper* 2007-01-4118.

Kim, Y. and Filipi, Z. (2007). Simulation Study of a Series Hydraulic Hybrid Propulsion System for a Light Truck. *SAE Technical Paper* 01-4151, 2007.

Matsuura, M., Korematsu, K., and Tanaka, J. (2004) Fuel Consumption Improvement of Vehicles by Idling Stop. *SAE Technical Paper* 01-1896.

Parker Runwise. Advanced Series Hybrid Drive (2013). HY34-1000, 03

Proclain Hydraulics. Addidrive Assist (2012), A31037L, 08.

Soriano, F., Alvarez-Florez, J., and Moreno-Eguilaz (2014), M. Experimentally Compared Fuel Consumption Modelling of Refuse Collecting Vehicles for Energy Optimization Purposes. *SAE Int. J. Commer. Veh.* 7(1):324-336.

Soriano, F., Moreno Eguilaz, M. and Alvarez-Florez, J. (2015). Drive cycle identification and energy demand estimation for refuse-collecting vehicles. *Vehicular Technology, IEEE Transactions on*, **64**, **11**, 4965-4973.

Surampudi, B., Nedungadi, A., Ostrowski, G., Montemayor, A. *et al*. (2009), Design and Control Considerations for a Series Heavy Duty Hybrid Hydraulic Vehicle, *SAE Technical Paper* 2009-01-2717.

Wadsley, L. (2011). Optimal system solutions enabled by Digital Pumps. *International Exposition for Power Transmission, IFPE, Las Vegas*.

Wohlgemuth, S., Wachtmeister, G., and Kloft, P (2013). Development of a Hydraulic Hybrid System for Urban Traffic. *SAE Technical Paper* 2013-01-1479.

Wu. B, Lin Ch., Filipi Z., Peng H., AssanisD.(2002) Optimization of Power Management Strategies for a Hydraulic Hybrid Medium Truck. *Proceedings of the 2002 Advanced Vehicle Control Conference*.

Wu B., Lin Ch., Filipi Z., Peng H., Assanis D. (2004) Optimal Power Management for a Hydraulic Hybrid Delivery Truck. *Vehicle System Dynamics - VEH SYST DYN* , 42, 1-2, 23-40.

Y. L. Chen, S. -A. Liu, J. -H. Jiang, T. Shang, Y. -K. Zhang, W. Wei (2013), Dynamic analysis of energy storage unit of the hydraulic hybrid vehicle, International Journal of Automotive Technology, 14, 101-112

Zhengce, C., WuS., Li M., Du, Ch. (2009). Series and Parallel Hybrid System Performance Comparison Based on the City bus Cycle. *Power and Energy Engineering Conference, 2009. APPEEC 2009. Asia-Pacific*, 1-5, 27-31.